WIDELY SEPARATED FREQUENCIES IN COUPLED OSCILLATORS WITH ENERGY-PRESERVING QUADRATIC NONLINEARITY

J.M. TUWANKOTTA

Abstract. In this paper we present an analysis of a system of coupled oscillators suggested by atmospheric dynamics. We make two assumptions for our system. The first assumption is that the frequencies of the characteristic oscillations are widely separated and the second is that the nonlinear part of the vector field preserves the distance to the origin. Using the first assumption, we prove that the reduced normal form of our system has an invariant manifold which exists for all values of the parameters. This invariant manifold cannot be perturbed away by including higher order terms in the normal form. Using the second assumption, we view the normal form as an energy-preserving three-dimensional system which is linearly perturbed. Restricting ourselves to a small perturbation, the flow of the energy-preserving system is used to study the flow in general. We present a complete study of the flow of the energy-preserving system and its bifurcations. Using these results, we provide the condition for having a Hopf bifurcation of one of the two equilibria of the perturbed system. We also numerically follow the periodic solution created via the Hopf bifurcation and find a sequence of Period-Doubling and Fold bifurcations, also a Torus bifurcation.

Keywords: High-order resonances, singular perturbation, bifurcation.

1. Introduction

High-order resonances in a system of coupled oscillators tend to get less attention rather than the lower-order ones. In fact, as noticed in [10], the tradition in engineering is to neglect the effect of high-order resonances in a system. However, the results of Broer et.al. [1, 2], Langford and Zhan [14, 15], Nayfeh et.al [16, 17], Tuwankotta and Verhulst [20]. etc., show that in the case of widely separated frequencies, which can be seen as an extreme type of high-order resonances, the behavior of the system is different from the expectation.

Think of a system

$$\begin{aligned} \ddot{x} + \omega_x x &= f(\dot{x}, x, y, t) \\ \ddot{y} + \omega_y y &= g(\dot{y}, x, y, t), \end{aligned}$$

where ω_x and ω_y are assume to be positive real numbers, and f and g are sufficiently smooth functions. If there exists $k_1,\ k_2 \in \mathbb{N}$ such that $k_1\omega_x - k_2\omega_y = 0$, we called the situation resonance. If k_1 and k_2 are relatively prime and $k_1 + k_2 < 5$ we call this *low-order resonance* (or, also called *genuine* or strong resonances).

One of the phenomena of interest in a system of coupled oscillators is the energy exchanges between the oscillators. It is well known that in low-order resonances, this happens rather dramatically compared to in higher-order ones. For systems with widely separated frequencies, the behavior is different from the usual high-order resonances in the following sense. In [10, 16, 17], the authors observed a large scale of energy exchanges between the oscillators. In the Hamiltonian case, the results in [1, 2, 20] show that although there is no energy exchange

between the oscillators, there are important phase interactions occurring on a relatively short time-scale.

1.1. **Motivations.** In this paper we study a system of coupled oscillators with widely separated frequencies. This system is comparable with the systems which are considered in [10, 14, 15, 16, 17]. However, we are mainly concerned with the internal dynamics. Thus, in comparison with [10, 16, 17], there is no time-dependent forcing term in our system. Our goal is to describe the dynamics of the model using normal form theory. This analysis can be considered as a supplement to [14, 15] which are concentrated on the unfolding of the trivial equilibrium and its bifurcation.

Another motivation for studying this system comes from the applications in atmospheric research. In [4], a model for ultra-low-frequency variability in the atmosphere is studied. In such a study, one usually encounters a system with a large number of degrees of freedom, which is a projection of the Navier-Stokes equation to a finite-dimensional space. The projected system in [4] is ten-dimensional and the projection is done using so-called *Empirical Orthogonal Functions* (see the reference in [4] for introduction to the EOF). In that projected system, the linearized system around an equilibrium has two among five pairs of eigenvalues of $\lambda_1 = -0.00272154 \pm i0.438839$ and $\lambda_5 = 0.00165548 \pm i0.0353438$. One can see that $\mathrm{Im}(\lambda_1)/\mathrm{Im}(\lambda_2) = 12.4163\ldots$, which is clearly not a strong resonance.

In fluid dynamics, the model usually has a special property, namely the nonlinear part of the vector field (the advection term) preserves the energy. We assume the same holds in our system. We take the simplest representation of the energy, that is the distance to the origin, and assume that the flow of the nonlinear part of our system preserves the distance to the origin.

The relation between a ten-dimensional, or even worse, an infinite-dimensional system of differential equations and a system consisting of only two special modes is an important question. However, it falls beyond the scope of this paper. In this paper we want to provide, as completely as possible, the information of the dynamics of a two coupled oscillators system having widely separated frequencies and an energy-preserving nonlinearity.

1.2. **Summary of the results.** Let us consider a system of first-order ordinary differential equations in $\mathbb{R}^4$ with coordinate $\boldsymbol{z} = (z_1, z_2, z_3, z_4)$. We add the following assumptions to our system.

- (A_1) The system has an equilibrium: $\boldsymbol{z}_\circ \in \mathbb{R}^4$ such that the linearized vector field around $\boldsymbol{z}_\circ$ has four simple eigenvalues $\lambda_1, \overline{\lambda_1}, \lambda_2$, and $\overline{\lambda_2}$, where $\lambda_1, \lambda_2 \in \mathbb{C}$. Furthermore, we assume that $\mathrm{Im}(\lambda_1)$ is much larger in size compared to $\mathrm{Im}(\lambda_2)$, $\mathrm{Re}(\lambda_1)$ and $\mathrm{Re}(\lambda_2)$.
- (A_2) The nonlinear part of the vector field preserves the energy which is represented by the distance to the origin.

In section 2, we will re-state these assumptions in a more mathematically precise manner.

We use normal form theory to construct an approximation for our system. In Theorem 3.1, we show that the normal form, truncated up to any finite degree, exhibits an invariant manifold which exists for all values of parameters. This invariant manifold coincides with the linear eigenspace corresponding to the pair of eigenvalues λ_2 and $\overline{\lambda_2}$.

We simplify the system even more by looking only at the situation where $\mathrm{Re}(\lambda_1)$ and $\mathrm{Re}(\lambda_2)$ are small. In fact, if $\mathrm{Re}(\lambda_1) = \mathrm{Re}(\lambda_2) = 0$, the system preserves the energy. The phase space of such a system is fibered by the energy manifolds, which are spheres in our case. By restricting the flow of the normal form to each of these spheres, we reduce the normal form to a two-dimensional system of differential equations parameterized by the value of the energy, which is the radius of the sphere. As a consequence, each equilibrium that we find on a particular sphere can be continued to some neighboring spheres. This gives us a continuous set of equilibria of the normal form for $\mathrm{Re}(\lambda_1) = \mathrm{Re}(\lambda_2) = 0$. In fact we have two of such sets in our system. This analysis is presented in sections 5 and 6.

For small values of $\mathrm{Re}(\lambda_1)$ and $\mathrm{Re}(\lambda_2)$, the normal form can be considered as an energy-preserving three-dimensional system which is linearly perturbed. The dynamics consists of slow-fast dynamics. The fast dynamics corresponds to the motion on two-spheres described in the above paragraph. The slow dynamics is the motion from one sphere to another along the direction of the curves of critical points.

In [7], Fenichel proved the existence of an invariant manifold where the slow dynamics takes place. This slow manifold is actually a perturbation of the manifold of equilibria which exists for the unperturbed case. The conditions that have to be satisfied are the unperturbed manifold should be normally hyperbolic and compact. Since both of such curves in our system, fail to satisfy these condition, we cannot conclude that there exists an invariant slow manifold. This situation is already realized in [12, 10]. We illustrate this in a simple example below.

Example 1.1. *Consider a system of differential equations*

$$\begin{aligned} \dot{x} &= x^2 \\ \varepsilon\dot{y} &= -y, \end{aligned}$$

with $\varepsilon \ll 1$. This system has an invariant manifold $y = 0$. The solutions of the system live in an integral curve defined by

$$y(x) = y_\circ \exp\left(\tfrac{1}{\varepsilon}\tfrac{x_\circ - x}{x_\circ x}\right)$$

where $(x_\circ, y_\circ)$ is the initial condition. For $x_\circ > 0$ the limiting behavior is different from one solution to another. In fact, as $x \to \infty$, $y \not\to 0$ (in this example x goes to infinity in finite time). Thus, a unique manifold to which all solutions are attracted does not exist. However, as $\varepsilon \downarrow 0$, the solutions become exponentially close to $y = 0$ for large x. This example is treated carefully in [21].

For an introduction to Geometric Singular Perturbation, see [12]. For a thorough treatment on the theory of invariant manifold, see [11] and also [22]. The dynamics however, is similar apart from the fact that the slow motion is tunneling into a very narrow tube along the curve instead of following a unique manifold. For instance in the example above, the width of the tunnel is $O(\exp(-1/\varepsilon x_\circ))$.

The linear perturbation is governed by two parameters: μ_1 $(= \mathrm{Re}(\lambda_1))$ and μ_2 $(= \mathrm{Re}(\lambda_2))$. If $\mu_1\mu_2 > 0$, the system becomes simple in the sense that we have only one equilibrium, the trivial one. The flow of the normal form collapses to the trivial equilibrium either in positive or negative time, which implies the non-existence of any other limit set. In the opposite case: $\mu_1\mu_2 < 0$, the trivial equilibrium is unstable. In a general situation, we have two critical points: the trivial one and the nontrivial one. There are two situations where the nontrivial

equilibrium fails to exist. The first situation is when we have no interaction between the dynamics of (z_1, z_2) and (z_3, z_4). The other situation corresponds to a particular instability balance between the modes. For a large part of the parameter space, we prove that the solutions are bounded (see section 4). Combining the information of the energy-preserving flow (section 5) and its bifurcations (section 6), we can derive a lot of information of the dynamics of the normal form for small μ_1 and μ_2.

The nontrivial equilibrium that we mentioned above, is a continuation of one of the equilibria of the fast system. Although we have the explicit expression for the location of the nontrivial equilibrium, to derive the stability result using linearization is still cumbersome. Using geometric arguments, the stability result and also the bifurcations of this nontrivial equilibrium can be achieved easily.

We show in this paper that the only possible bifurcation for the nontrivial equilibrium is Hopf bifurcation. This Hopf bifurcation can be predicted analytically. This result is presented in section 8. We also study the bifurcation of the periodic solution which is created via the Hopf bifurcation of the nontrivial equilibrium. However, this is difficult to do analytically. Using the continuation software AUTO [5], we present the numerical bifurcation analysis of this periodic solution in section 9. Numerically, we find Torus bifurcation and a sequence of Period-Doubling and Fold bifurcations.

1.3. **The lay out.** In section 2 the system is introduced. The small parameter in the system is the frequency of one of the oscillators and it is called $\tilde{\varepsilon}$. Using averaging we normalize the system and reduce it to a three-dimensional system of differential equations. The normalized system is analyzed in section 3. We complete the analysis of the case where $\mu_1\mu_2 > 0$ in this section and assume that $\mu_1\mu_2 < 0$ in the rest of the paper. In section 4, we re-scale μ_1 and μ_2 using a new small parameter ε. By doing this we formulate the normal form as a perturbation of an energy-preserving system in three-dimensional space. There are two continuous sets of equilibria of the energy-preserving part of the system and they are analyzed in section 5. In section 6, we use the fact that the phase space of the energy-preserving part of the system is fibered by invariant half spheres, to project the unperturbed system to a two-dimensional system of differential equations. The stability results derived in section 5, are applied to study the bifurcation in the projected system. In section 7, we turn on our perturbation parameter: $\varepsilon \neq 0$. Using geometric arguments, we derive the stability results for the nontrivial equilibrium. Furthermore, in section 8 we use a similar argument to derive the condition for Hopf bifurcation of the nontrivial equilibrium. The bifurcation of the periodic solution which is created via Hopf bifurcation, is studied numerically in section 9.

2. Problem formulation and normalization

Let $0 < \tilde{\varepsilon} \ll 1$ be a small parameter. Consider a system of ordinary differential equations in $\mathbb{R}^4$ with coordinates $\boldsymbol{z} = (z_1, z_2, z_3, z_4)$, defined by:

$$\dot{\boldsymbol{z}} = \begin{pmatrix} A_1 & 0 \\ 0 & A_2 \end{pmatrix} \boldsymbol{z} + \boldsymbol{F}(\boldsymbol{z}), \tag{2.1}$$

where A_j, $j = 1, 2$ are two by two matrices, with eigenvalues: $\tilde{\varepsilon}\mu_1 \pm i$, and $\tilde{\varepsilon}\mu_2 \pm i\tilde{\varepsilon}\omega$, ω, μ_1, and μ_2 are real numbers. We assume that μ_1 and μ_2 are bounded and ω is bounded away from zero and infinity. The nonlinear function $\boldsymbol{F}$ is a quadratic, homogeneous polynomial in

$\boldsymbol{z}$ satisfying: $\boldsymbol{z} \cdot \boldsymbol{F}(\boldsymbol{z}) = 0$. Thus, the flow of the system $\dot{\boldsymbol{z}} = \boldsymbol{F}(\boldsymbol{z})$ is tangent to the sphere: ${z_1}^2 + {z_2}^2 + {z_3}^2 + {z_4}^2 = R^2$ where R is the radius.

We re-scale the variables by $\boldsymbol{z} \mapsto \tilde{\varepsilon}\boldsymbol{z}$. By doing this we formulate the system (2.1) as a perturbation problem, i.e.

$$\dot{\boldsymbol{z}} = \begin{pmatrix} \bar{A}_1 & 0 \\ 0 & 0 \end{pmatrix} \boldsymbol{z} + \tilde{\varepsilon}\bar{\boldsymbol{F}}(\boldsymbol{z}), \tag{2.2}$$

with $\bar{A}_1 = \begin{pmatrix} 0 & 1 \\ -1 & 0 \end{pmatrix}$. Note that $\bar{\boldsymbol{F}}$ is no longer homogeneous; it contains linear terms. We normalize (2.2) with respect to the actions defined by the flow of the *unperturbed* vector field of (2.2) (that is for $\tilde{\varepsilon} = 0$). This can be done by applying the transformation

$$z_1 \mapsto r\cos(t+\varphi), z_2 \mapsto -r\sin(t+\varphi), z_3 \mapsto x \text{ and } z_4 \mapsto y$$

to (2.2) and then average the resulting equations of motion with respect to t over 2π. See [18] for details on the averaging method.

The averaged equations are of the form

$$\begin{aligned} \dot{\varphi} &= \tilde{\varepsilon}G_1(r,x,y) + O(\tilde{\varepsilon}^2) \\ \dot{r} &= \tilde{\varepsilon}G_2(r,x,y) + O(\tilde{\varepsilon}^2) \\ \dot{x} &= \tilde{\varepsilon}G_3(r,x,y) + O(\tilde{\varepsilon}^2) \\ \dot{y} &= \tilde{\varepsilon}G_4(r,x,y) + O(\tilde{\varepsilon}^2), \end{aligned}$$

where $G_j, j = 1, \ldots, 4$ are at most quadratic. Thus, we can reduce the system to a three-dimensional system of differential equations by dropping the equation for φ. This reduction is typical for an autonomous system. We note that by applying the averaging method, we can preserve the energy-preserving nature of the nonlinearity. Furthermore, by rotation we can choose a coordinate system such that the equation for r is of the form $\dot{r} = \tilde{\varepsilon}\tilde{G}_2(r,x) + O(\tilde{\varepsilon}^2)$.

We omit the details of the computations and just write down the reduced averaged equations (or normal form) after rescaling time by $t \mapsto \tilde{\varepsilon}t$, i.e.

$$\begin{pmatrix} \dot{r} \\ \dot{x} \\ \dot{y} \end{pmatrix} = \begin{pmatrix} \mu_1 & 0 & 0 \\ 0 & \mu_2 & 0 \\ 0 & 0 & \mu_2 \end{pmatrix} \begin{pmatrix} r \\ x \\ y \end{pmatrix} + \begin{pmatrix} \delta x r \\ \Omega(x,y)y - \delta r^2 \\ -\Omega(x,y)x \end{pmatrix}, \tag{2.3}$$

where $\Omega(x,y) = \omega + \alpha x + \beta y$, $\mu_1, \mu_2, \alpha, \beta, \omega$, and δ are real numbers. It is important to note that up to this order, the small parameter $\tilde{\varepsilon}$ is no longer present in the normal form, by time reparameterization.

To facilitate the analysis we introduce some definitions. Let a function $\boldsymbol{G} : \mathbb{R}^3 \to \mathbb{R}^3$ be defined by:

$$\boldsymbol{G}(\boldsymbol{\xi}) = \begin{pmatrix} \delta x r \\ \Omega(x,y)y - \delta r^2 \\ -\Omega(x,y)x \end{pmatrix}, \tag{2.4}$$

where $\boldsymbol{\xi} = (r,x,y)^T$, $\Omega(x,y) = \omega + \alpha x + \beta y$. We also define a function $\mathcal{S} : \mathbb{R}^3 \to \mathbb{R}$ by

$$\mathcal{S}(\boldsymbol{\xi}) = r^2 + x^2 + y^2. \tag{2.5}$$

Note that $\frac{d}{dt}(\mathcal{S}) = 0$ along the solution of $\dot{\boldsymbol{\xi}} = \boldsymbol{G}(\boldsymbol{\xi})$. Lastly, we define

$$S(R) = \{\boldsymbol{\xi} \mid r^2 + x^2 + y^2 = R^2, R \geq 0\} \tag{2.6}$$

which is the level set $\mathcal{S}(\boldsymbol{\xi}) = R^2$.

Remark 2.1 (Symmetries in the system)**.** *We consider two types of transformations: transformation in the phase space $\Phi_j : \mathbb{R}^3 \to \mathbb{R}^3$, $j = 1, 2$ and in the parameter space: $\Psi : \mathbb{R}^6 \to \mathbb{R}^6$. Consider $\Phi_1(r, x, y) = (-r, x, y)$, which keeps the system (2.3) invariant. This immediately reduces the phase space to $\mathcal{D} = \{r \geq 0 | r \in \mathbb{R}\} \times \mathbb{R}^2$. Another symmetry which turns out to be important is a combination between $\Phi_2(r, x, y) = (r, -x, -y)$ and $\Psi(\alpha, \beta, \delta, \omega, \mu_1, \mu_2) = (-\alpha, -\beta, -\delta, \omega, \mu_1, \mu_2)$. System (2.3) is invariant if we transform the variables using Φ_2 and also the parameters using Ψ. It implies that we can reduce the parameter space by fixing a sign for β. We choose $\beta < 0$. One can also consider a combination involving time-reversal symmetry. We are not going to take this symmetry into account because this symmetry changes the stability of all invariant structures in the system. Thus, we assume: $\omega > 0$.*

3. General invariant structures

System (2.3) has exactly two general invariant structures in the sense that they exist for all values of the parameters. They are the trivial equilibrium $(r, x, y) = (0, 0, 0)$ and the invariant manifold $r = 0$. The linearized system around the trivial equilibrium has eigenvalues μ_1, $\mu_2 \pm i\omega$. We have three cases: $\mu_1\mu_2 > 0$, $\mu_1\mu_2 < 0$ or $\mu_1\mu_2 = 0$.

If $\mu_1\mu_2 > 0$, along the solutions of system (2.3), we have $\dot{\mathcal{S}} = \mu_1 r^2 + \mu_2(x^2+y^2)$ (see (2.5) for the definition of $\mathcal{S}$) is positive (or negative) semi-definite if $\mu_1 > 0$ (or $\mu_1 < 0$, respectively). Thus, $\mathcal{S}$ is a globally defined Lyapunov function. As a consequence, all solutions collapse into the neighborhood of the trivial equilibrium for positive (or negative) time , if $\mu_1 < 0$ (or $\mu_1 > 0$, respectively). Moreover, there is no other invariant structure apart from this trivial equilibrium and the invariant manifold $r = 0$. This completes the analysis for this case.

For $\mu_1\mu_2 < 0$ the trivial equilibrium is unstable. In the case where $\mu_1 > 0$, the equilibrium has one dimensional unstable manifold and two dimensional stable manifold. The stable manifold is the invariant manifold $r = 0$. The situation is reversed in the case $\mu_1 < 0$. The global dynamics in this case is not clear at the moment. We will come back to this question in the sections 7, 8 and 9.

For $\mu_1\mu_2 = 0$, we have again three different possibilities: $\mu_1 = 0$, or $\mu_2 = 0$ or $\mu_1 = \mu_2 = 0$. For the purpose of this paper, we consider only the most degenerate case: $\mu_1 = \mu_2 = 0$. In this case, $\dot{\mathcal{S}} = 0$ which means $S(R)$ is invariant under the flow of (2.3). Thus, the trivial equilibrium is neutrally stable. The phase space of system (2.3) is fibered by invariant sphere $S(R)$ and hence the flow reduces to a two-dimensional flow on these spheres.

The second invariant is the invariant manifold $r = 0$. The following theorem gives us the existence of this manifold.

Theorem 3.1 (The existence of an invariant manifold)**.** *Consider system (2.1), i.e.*

$$\dot{\boldsymbol{z}} = \begin{pmatrix} A_1 & 0 \\ 0 & A_2 \end{pmatrix} \boldsymbol{z} + \boldsymbol{F}(\boldsymbol{z}), \tag{3.1}$$

with $\boldsymbol{z} \in \mathbb{R}^4$, $\boldsymbol{F} : \mathbb{R}^4 \to \mathbb{R}^4$ is sufficiently smooth with properties: $\boldsymbol{F}(\boldsymbol{0}) = \boldsymbol{0}$ and $D_{\boldsymbol{z}}\boldsymbol{F}(\boldsymbol{0})$ is a zero matrix. The eigenvalues of A_1 are: $\tilde{\varepsilon}\mu_1 \pm i$ while for A_2 are: $\tilde{\varepsilon}\mu_2 \pm i\tilde{\varepsilon}\omega$, where $\omega, \mu_j \in \mathbb{R}$, $j = 1, 2$ and $0 < \tilde{\varepsilon} \ll 1$. Let $\dot{\boldsymbol{z}} = \overline{\boldsymbol{F}}_k(\boldsymbol{z})$ be a normal form for (3.1), up to an arbitrary finite degree k. The flow of the normal form keeps the manifold $\mathcal{M} = \{\boldsymbol{z} \mid {z_1}^2 + {z_2}^2 = 0\}$ invariant.

Proof. Let us transform the coordinate by $\boldsymbol{z} \mapsto \tilde{\varepsilon}\boldsymbol{z}$. System (3.1) is transformed to

$$\dot{\boldsymbol{z}} = \mathrm{diag}(\bar{A}_1, 0)\boldsymbol{z} + \tilde{\varepsilon}\bar{\boldsymbol{F}}(\boldsymbol{z}; \tilde{\varepsilon}),$$

where $\bar{\boldsymbol{F}}$ contains also linear term. Consider the algebra of vector fields in $\mathbb{R}^4$: $\mathcal{X}(\mathbb{R}^4)$. Note that we can view the vector field X as a map $X : \mathbb{R}^4 \to \mathbb{R}^4$. The Lie bracket in this algebra is the srandard commutator between vector fields, i.e.

$$[X_1, X_2](\boldsymbol{z}) = dX_1(\boldsymbol{z}) \cdot X_2(\boldsymbol{z}) - dX_2(\boldsymbol{z}) \cdot X_1(\boldsymbol{z}),$$

where $X_1, X_2 \in \mathcal{X}(\mathbb{R}^4)$ and $\boldsymbol{z} \in \mathbb{R}^4$. Let the unperturbed vector field of (2.2) be denoted by $X_\circ$. It defines a linear rotation in (z_1, z_2)-plane. This action keeps all points in the manifold $\mathcal{M} = \{\boldsymbol{z} | {z_1}^2 + {z_2}^2 = 0\}$ invariant. We normalize the vector field corresponding to the system $\dot{\boldsymbol{z}} = \tilde{\varepsilon}\bar{F}(\boldsymbol{z})$ with respect to this rotation. The resulting normalized vector field truncated to a finite order k: $X_{\tilde{F}}$, commutes with $X_\circ$. Thus $[X_\circ, X_{\tilde{F}}] = 0$. In particular, for every $m \in \mathcal{M}$,

$$0 = [X_\circ, X_{\tilde{F}}](m) = dX_\circ(m) \cdot X_{\tilde{F}}(m) - dX_{\tilde{F}}(m) \cdot X_\circ(m) = dX_\circ(m) \cdot X_{\tilde{F}}(m).$$

This implies $X_{\tilde{F}}(m) \in \ker(dX_\circ(m)) = \mathcal{M}$. □

The dynamics in this invariant manifold gives us only a partial information of the flow. In the next section we re-write (2.3) as a perturbation of a system with a first integral.

4. The rescaled system

Recall that if $\mu_1 = \mu_2 = 0$, system (2.3) has an integral, i.e. $\mathcal{S}(\boldsymbol{\xi})$. Let ε be a small parameter. We re-scale: $\mu_1 = \varepsilon\kappa_1$ and $\mu_2 = -\varepsilon\kappa_2$ with $\kappa_1\kappa_2 > 0$. System (2.3) becomes

$$\begin{aligned} \dot{r} &= \delta x r + \varepsilon\kappa_1 r \\ \dot{x} &= \Omega y - \delta r^2 - \varepsilon\kappa_2 x \\ \dot{y} &= -\Omega x - \varepsilon\kappa_2 y, \end{aligned} \tag{4.1}$$

where $\Omega = \omega + \alpha x + \beta y$. We have assumed that $\omega > 0$ and $\beta < 0$.

Lemma 4.1. *All solutions of system (4.1) with $\delta > 0$, $\kappa_1 > 0$ and $\kappa_2 > 0$ are bounded.*

Proof. Consider a function $F(\boldsymbol{\xi}) = r^2 + x^2 + y^2 - 2\eta(\beta x - \alpha y)$ where η is a parameter to be determined later. The level set of F, i.e. $F(r, x, y) = c$ is a sphere, centered at $(r, x, y) = (0, \eta\beta, -\eta\alpha)$ with radius $\sqrt{c + \eta^2(\alpha^2 + \beta^2)}$. The derivative of F along a solution of system (4.1) is

$$\mathcal{L}_t F = (2\varepsilon\kappa_1 + 2\eta\beta\delta) r^2 - \varepsilon\kappa_2 \left(x^2 + y^2\right) - 2\eta(\alpha x + \beta y)^2 - L(x, y),$$

where $L(x, y)$ is a polynomial with degree at most one. Since $\kappa_1 > 0$, $\kappa_2 > 0$ and $\delta > 0$, we have: $2\varepsilon\kappa_1 + 2\eta\beta\delta < 0$ if and only if $\eta > -\varepsilon\kappa_1/(\beta\delta) > 0$. This means under the conditions in this Lemma, we can always choose η in such a way that the quadratic part of $\mathcal{L}_t F$ is negative definite. This ends the proof. □

Let us fix η so that the quadratic part of $\mathcal{L}_t F$ is negative definite. Consider $(x, y) \in \mathbb{R}^2$ and a real number $c \in \mathbb{R}$. From equation $r^2 + (x - \eta\alpha)^2 + (y + \eta\alpha) = c + \eta^2\left(\alpha^2 + \beta^2\right)$ we can compute r which solves the equation, as a function of x, y, and c: $r(x, y; c)$. Let us define $G : \mathbb{R}^2 \to \mathbb{R}$, by assigning to (x, y) the value of $(\mathcal{L}_t F)(r(x, y; c), x, y)$. One can check that $G(x, y)$ has a unique maximum and $\partial G/\partial c$ does not depend on x or y. Thus, we can solve $\partial G/\partial x = 0$ and $\partial G/\partial y = 0$ for (x, y), and the solution is independent of c. Let $(x_\circ, y_\circ)$ be the solution of $\partial G/\partial x = 0$ and $\partial G/\partial y = 0$. We can solve the equation $G(x_\circ, y_\circ; c) = 0$ for c and let's call the solution $c_\circ$. Clearly, $G(x, y; c_\circ) \leq 0$. Therefore, for the chosen value of η, the

ball: $\mathcal{B} = \{(r,x,y) \mid r^2 + (x-\eta\beta)^2 + (y+\eta\alpha)^2 \leq c_\circ + \eta^2\left(\alpha^2+\beta^2\right)\}$, is invariant under the flow of system (4.1). Moreover, the vector field of system (4.1) is always pointing inward at the boundary of the ball except probably at one point where $G(x,y;c_\circ)=0$. We summarize in the following corollary.

Corollary 4.2. *All solutions of (4.1) for $\delta > 0$, $\kappa_1 > 0$ and $\kappa_2 > 0$, after some time stay inside the ball $\mathcal{B}$.*

We cannot apply the same arguments as above if $\delta < 0$. In section 7 we will derive the conditions for bounded solutions in this case. If $\delta = 0$, then the dynamics of r is decoupled from the rest. Moreover, r grows exponentially with a rate: $\varepsilon\kappa_1$. Thus, we conclude that all solutions except for those in $r = 0$, eventually run off to infinity. If $\kappa_1 < 0$ and $\kappa_2 < 0$, in the invariant manifold $r = 0$ all solutions run off to infinity accept for the origin. This motivates us to restrict our self to the case where $\kappa_1 > 0$ and $\kappa_2 > 0$. To understand system (4.1), first we study the case where $\varepsilon = 0$.

5. Two continuous sets of equilibria

Recall that we have assumed that $\omega > 0$ and $\beta < 0$ (see remark 2.1). For $\varepsilon = 0$, system (4.1) becomes

$$\begin{aligned} \dot{r} &= \delta x r \\ \dot{x} &= \Omega y - \delta r^2 \\ \dot{y} &= -\Omega x. \end{aligned} \tag{5.1}$$

At this point we assume that $\alpha \neq 0$, $\delta \neq 0$, $\beta < 0$, and $\omega > 0$.

5.1. **A continuous set of equilibria in the plane $r = 0$.** There are two continuous sets of equilibria in system (5.1). One of them is the line: $\Omega = \omega + \alpha x + \beta y = 0$ and it lies in the invariant manifold $r = 0$. We parameterize this set by $y = y_\circ$, i.e.

$$(r,x,y) = \left(0, -\frac{\beta y_\circ + \omega}{\alpha}, y_\circ\right), \quad y_\circ \in (-\infty, +\infty). \tag{5.2}$$

The eigenvalues of system (5.1) linearized around (5.2), are:

$$\lambda_1 = 0, \lambda_2 = -\frac{\delta(\beta y_\circ + \omega)}{\alpha}, \text{ and } \lambda_3 = \frac{(\alpha^2+\beta^2)y_\circ + \beta\omega}{\alpha}. \tag{5.3}$$

It is clear that λ_1 is the eigenvalue corresponding to the tangential direction to the set (5.2). The behavior of the linearized system around the equilibria in (5.2) is determined by the eigenvalues (5.3). They are presented in figure 1

Remark 5.1. *If $\alpha = 0$ we parameterize the continuous set as $(r,x,y) = (0, x_\circ, -\omega/\beta)$, $\quad x_\circ \in (-\infty, +\infty)$. Each of these equilibria with $x_\circ > 0$ has two positive eigenvalues (and one zero) and those with $x_\circ < 0$ have two negative eigenvalues (and one zero). At $x_\circ = 0$ we have two extra zero eigenvalues.*

5.2. **A continuous set of equilibria in the plane $x = 0$.** The other continuous set of equilibria of system (5.1) lies in the plane $x = 0$. The set is a curve defined by equation $\delta r^2 - \beta\left(y + \omega/(2\beta)\right)^2 = -\omega^2/(4\beta)$, which is an ellipse if: $\delta > 0$, or hyperbola if $\delta < 0$. This curve intersects $r = 0$ at $y = 0$ and at $y = -\omega/\beta$. Note that $y = -\omega/\beta$ is also the intersection point of the curve with the line $\Omega = 0$ which explains why we have an extra zero eigenvalue if $y_\circ = -\omega/\beta$ in (5.3).

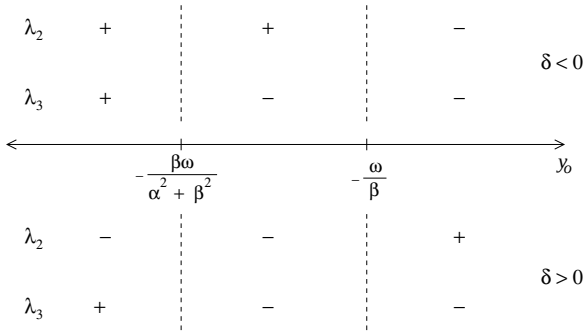

FIGURE 1. The above diagram shows the sign of the eigenvalues (5.3) for $\alpha < 0$.

5.2.1. *An ellipse of critical points.* Let us now look at the case of $\delta > 0$ where we have an ellipse of critical points. We parameterize the ellipse by $y_\circ$, i.e.

$$(r, x, y) = \left(\sqrt{\frac{y_\circ(\omega + \beta y_\circ)}{\delta}}, 0, y_\circ \right) \tag{5.4}$$

where $0 \le y_\circ \le -\omega/\beta$. The linearized system of system (5.1) around each of these equilibria has eigenvalues $\lambda_1 = 0$, and $\lambda_{2,3} = \frac{1}{2}(\alpha y_\circ \pm \sqrt{D})$ where

$$D = (\alpha y_\circ)^2 - 4(\omega + \beta y_\circ)(2(\delta + \beta)y_\circ + \omega) \tag{5.5}$$

The following lemma gives the stability results for these critical points.

Lemma 5.2. *Let $\alpha < 0$.*

1. *If $\delta \ge -\beta/2$ then $\Re(\lambda_{2,3}) < 0$ for all except the two end points of the set of equilibria (5.4).*
2. *If $0 < \delta < -\beta/2$, then at the equilibrium*

$$(r_s, x_s, y_s) = \left(-\frac{\omega}{2(\delta+\beta)} \sqrt{-\frac{\beta + 2\delta}{\delta}}, 0, -\frac{\omega}{2(\delta+\beta)} \right), \tag{5.6}$$

$\lambda_2 = 2\alpha y_\circ < 0$ and $\lambda_3 = 0$. Moreover, for the equilibria in (5.4) with $0 < y_\circ < y_s$, $\Re(\lambda_{2,3}) < 0$, while for the other equilibria ($y_s < y_\circ < -\omega/\beta$), $\lambda_2 < 0$ and $\lambda_3 > 0$.

Proof. Consider D in (5.5) as a quadratic function in $y_\circ$. If $D(y_\circ) < 0$ for $0 < y_\circ < -\beta/\omega$ then the Lemma holds. Let $D > 0$ and define a function $L(y_\circ) = \left((\alpha y_\circ)^2 - D(y_\circ)\right)/4 = (\omega + \beta y_\circ)(2(\delta + \beta)y_\circ + \omega)$. Note that $L(0) = \omega^2 > 0$ and $L(-\omega/\beta) = 0$. If $\delta \ge -\beta/2$ we have $L'(-\omega/\beta) = -(2\delta + \beta)\omega \ge 0$. Thus we conclude that $D(y_\circ) > (\alpha y_\circ)^2$, for $0 < y_\circ < -\omega/\beta$. If $\delta > -\beta/2$, then $L'(-\omega/\beta) < 0$. Thus, there exists $0 < y_s < -\omega/\beta$ such that $L(y_s) = 0$. From the definition of $L(y_\circ)$ we conclude that $y_s = -\omega/\left(2(\delta + \beta)\right)$. Since $L(y_s) = 0$ we have $D(y_s) = (\alpha y_s)^2$ so that either $\lambda_2 = 0$ or $\lambda_3 = 0$. Moreover, $L'(y_s) < 0$ so that for $0 < y_\circ < y_s$, $L(y_\circ) > 0$. □

5.2.2. *A hyperbola of critical points.* For the case $\delta < 0$, the set of equilibria (5.4) is a hyperbola with two branches. We call the branch of the hyperbola with $y_\circ > -\omega/\beta$: the *positive*

branch and the one with $y_\circ < 0$: the *negative branch*. Recall that the eigenvalues of these equilibria are

$$\lambda_1 = 0, \lambda_2 = \frac{\alpha y_\circ + \sqrt{D}}{2}, \text{ and } \lambda_3 = \frac{\alpha y_\circ - \sqrt{D}}{2},$$

where $D = (\alpha y_\circ)^2 - 4(\omega + \beta y_\circ)(2(\delta + \beta)y_\circ + \omega)$. One can see that D is a quadratic function in $y_\circ$. It is easy to check that $\lambda_2 = 0$ or $\lambda_3 = 0$ if and only if $y_\circ = -\omega/\beta$ of $y_\circ = -\omega/2(\delta + \beta)$. However, for $\delta < 0$ we have $0 < -\omega/2(\delta+\beta) < -\omega/\beta$. Thus, we conclude that these equilibria cannot have an extra zero eigenvalue except for $y_\circ = -\omega/\beta$. Thus, at one of the branches, $\Re(\lambda_{2,3})$ are always negative while at the other branches positive. If $\alpha^2 < 8\beta(\delta + \beta)$ then for a large value of $y_\circ$, the eigenvalues are complex pair.

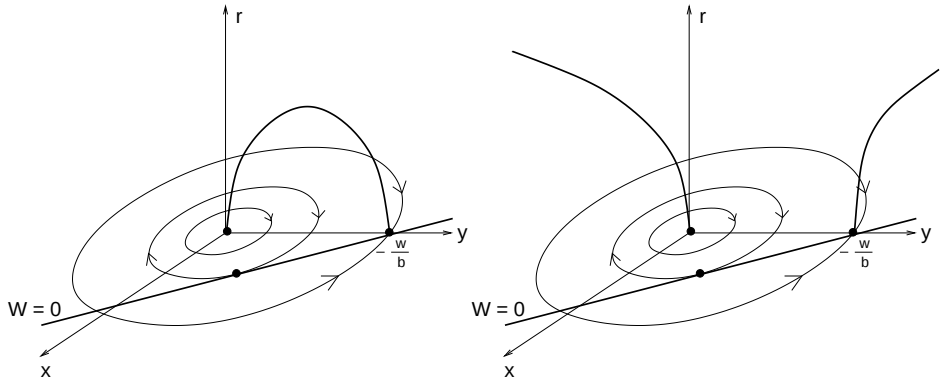

FIGURE 2. In this figure, the limit sets of system (5.1) are presented. The left plot is for the case of $\delta > 0$ and the right is for $\delta < 0$.

6. Bifurcation analysis of the energy-preserving system

Since $S(R)$ is invariant under the flow of system (5.1), we reduce it to a two-dimensional flow on a sphere. Moreover, the upper half of the sphere $S(R)$ is invariant under the flow of system (5.1). Thus we can define a bijection which maps orbits of system (5.1) to orbits of a two-dimensional system defined in a disc $D(\mathbf{0}, R) = \{(x, y)|x^2 + y^2 \leq {R_\circ}^2\}$. This bijection is nothing but a projection from the upper half of the sphere $S(R)$ to the horizontal plane. The transformed system is

$$\begin{aligned} \dot{x} &= \Omega y - \delta\left(R^2 - \left(x^2 + y^2\right)\right) \\ \dot{y} &= -\Omega x, \end{aligned} \tag{6.1}$$

where $\Omega = \omega + \alpha x + \beta y$. Note that the boundary of $D(\mathbf{0}, R)$: $x^2 + y^2 = R^2$ is invariant under the flow of system (6.1). We call this boundary *the equator*.

Let $R_p = -\omega/\beta$, $R_h = \omega/\sqrt{\alpha^2 + \beta^2}$ and

$$R_s = -\tfrac{\omega}{2(\delta+\beta)}\sqrt{\tfrac{2\beta+3\delta}{\beta+\delta}}.$$

These points are bifurcation points of system (6.1), as we vary R. It is easy to see that $R_h < R_p < R_s$ if all parameters are nonzero (recall that we have chosen $\beta < 0$).

6.1. **On the periodic solution of the projected system.** For $R < R_h$, the equator is a periodic solution. The period of this periodic solution at the equator is

$$T(R) = 4\int_0^R \frac{1}{\left(\omega+\alpha(R^2-y^2)+\beta y\sqrt{R^2-y^2}\right)}dy. \tag{6.2}$$

To study the stability of the periodic solution we transform to polar coordinate (ρ,θ) in the usual way. System (6.1) is transformed to

$$\begin{aligned}\dot\rho &= \delta(\rho^2-R^2)\cos(\theta)\\ \dot\theta &= -\omega-\alpha\rho\cos(\theta)-\left(\beta\rho+\delta\rho-\tfrac{\delta R^2}{\rho}\right).\end{aligned}$$

We then compute $\rho' = d\rho/d\theta = F(\rho,\theta)$, linearized it around $\rho = R$, to have a first order differential equation of the form $\rho' = A(\theta)\rho$. Near the periodic solution (i.e. $\rho = R$), $\theta(t)$ is monotonically increasing. Thus, $\rho' = A(\theta)\rho$ can be approximated by $\rho' = A^\circ\rho$ where

$$A^\circ = \int_0^{2\pi} A(\theta)d\theta = \alpha\delta\,\tfrac{4\pi^2\omega(-1+p^2+\sqrt{1-p^2})}{(\alpha^2+\beta^2)^{3/2}(-1+p^2)}, \tag{6.3}$$

and $p = R\sqrt{\alpha^2+\beta^2}/\omega$. Thus the periodic solution $x^2+y^2 = R^2$ is unstable if $\alpha\delta < 0$ or stable if $\alpha\delta > 0$. If $\alpha \neq 0$, then this periodic solution is the only periodic solution in the projected system (6.1).

Theorem 6.1. *If $\alpha \neq 0$, system (6.1) has no periodic solution in the interior of $D(\mathbf{0},R)$.*

Proof. Let us fix $R < R_p$. Then there is a unique equilibrium of system (6.1) in the interior of $D(\mathbf{0},R)$, namely: $(0,y_\circ)$. Define $\mathcal{I} = \{(0,y)|y_\circ < y \le R\}$ and $\mathcal{J} = \{(0,y)|-R \le y < y_\circ\}$. We write $\nu(x,y)$ for the velocity vector field corresponds to system (6.1). If $\Phi(t;(\bar x,\bar y))$ is the flow of system (6.1) at time t with initial condition $(\bar x,\bar y)$, we want to show that:

$$\text{for all } P\in\mathcal{J},\ \text{there exists } t_P\in(0,\infty) \text{ such that } \Phi(t_P;P)\in\mathcal{I}.$$

Let $\mathcal{J}'$ be a maximal subset of $\mathcal{J}$ with such a property. Clearly $\mathcal{J}' \neq \emptyset$ since $\Phi(T;(0,-R)) = (0,R)\in\mathcal{I}$ where $T<\infty$ is defined in (6.2). Take $(0,\bar y)\in\mathcal{J}'$ arbitrary, writing $\Phi(t;(0,\bar y)) = (x(t),y(t))$, there exists $\bar t$ such that $x(\bar t) = 0$. If $x(\bar t) = 0$, we have $\dot y(\bar t) = 0$, and $\dot x(\bar t)\neq 0$ (otherwise the equilibrium is not unique). By the Implicit Function Theorem we have: for an open neighborhood $\mathcal{N}$ of $(0,\bar y)$ there exists t (in the neighborhood of $\bar t$) such that $x(t) = 0$. Thus, $\mathcal{J}'$ is open in $\mathcal{J}$. $\mathcal{J}'$ is also closed by uniqueness of the equilibrium and the fact that $(0,-R)\in\mathcal{J}'$. Thus, we conclude that $\mathcal{J}' = \mathcal{J}$ (from the definition, $\mathcal{J}$ is connected).
Let us define a map $X:\mathbb{R}^2\to\mathbb{R}^2$ by $X(x,y) = (-x,y)$. Consider $\Gamma(t)$ which is the trajectory $(x(t),y(t)) = \Phi(t;P)$, $0\le t\le s$ where $P\in\mathcal{J}$ and $\Phi(s;P)\in\mathcal{I}$. Consider $t_\circ > 0$ such that $\Gamma(t_\circ) = (x,y)$ with $x\neq 0$. We have

$$\begin{aligned}\tfrac{d}{dt}X(\Gamma(t))\,|_{t=t_\circ} &= X\left(\tfrac{d}{dt}\Gamma(t)\big|_{t=t_\circ}\right) = X(\tfrac{d}{dt}\Phi(t_\circ;P)) = X(\nu(x,y))\\ &= -\nu(-x,y)+2\alpha x(x,-y)^T = -\nu(X(\Gamma(t)|_{t=t_\circ})+2\alpha x(x,-y)^T.\end{aligned}$$

Thus the vector field of system (6.1) is nowhere tangent to $X(\Gamma)$ accept if $\alpha = 0$.
Finally, consider the domain with boundary $\Gamma\cup X(\Gamma)$. The flow of system (6.1) is either flowing into the domain, or flowing out of the domain. We can make the domain as small as we want by choosing P close enough to $(0,y_\circ)$ or as big as possible by choosing P close enough to $(0,-R)$. We conclude that there is no other limit cycle in the interior of $D(\mathbf{0},R)$.
Let $R_\circ > R_p$. If $\delta > -\beta/2$, we can use Poincaré idea on the index of a vector field. Using this idea, the existence of a limit cycle implies the existence of an extra critical point. System

(6.1) has no other critical points apart from those in the equator. Thus, the limit cycle could not exists. This idea also applicable in the case $0 < \delta < -\beta/2$ and $R_\circ > R_s$. If $R_p < R_\circ < R_s$ is similar with the case $R_\circ < R_p$. □

Corollary 6.2. *If $\alpha = 0$ all but the critical solution of (6.1) for $R < R_h$ are periodic.*

Remark 6.3. The Bounded-Quadratic-Planar systems
In 1966, Coppel proposed a problem of identifying all possible phase-portrait of the so-called Bounded-Quadratic-Planar systems. A Bounded-Quadratic-Planar system is a system of two autonomous, ordinary, first order differential equations with quadratic nonlinearity where all solutions are bounded. The maximum number of limit cycles that could exists is one of the questions of Coppel. This problem turns out to be very interesting and not as easy as it seems. In fact, the answer to this problem contains the solution to the 16th Hilbert problem which is unsolved up to now (see [6]*). System (6.1) is a Bounded-Quadratic-Planar system. From this point of view, Theorem 6.1 is an important result for our systems. This result enables us to compute all possible phase portraits of system (6.1).*

From the previous section, one could guess that there are three situations for system (6.1), i.e. if $\delta > -\beta/\omega$, $0 < \delta < -\omega/2$, and $\delta < 0$. For R close to zero but positive, the phase portrait of system (6.1), is similar in all three situations. The equator is an unstable periodic solution and there is only one equilibrium of system (6.1). There are three possible bifurcations of the equilibria in system (6.1), namely simultaneous Saddle-Node and Homoclinic bifurcation, Pitchfork bifurcation and Saddle-Node bifurcation.

6.2. **A simultaneous Saddle-Node and Homoclinic bifurcation.** If R passes the value R_h, system (6.1) undergoes a simultaneous Saddle-Node and Homoclinic bifurcation (also called Andronov and Leontovich bifurcation, see [13] pp. 250-252). If $R < R_h$ the equator is a periodic solution. The period of this periodic solution goes to infinity as R approaches R_h from below. Exactly at $R = R_h$ the limit cycle becomes an homoclinic to a degenerate equilibrium (with one zero eigenvalue). This degenerate equilibrium is created via a Saddle-Node bifurcation. This is clear since after the bifurcation (that is when $R > R_h$) we have two equilibria in the equator and the homoclinic orbit vanishes.

This bifurcation occurs in all three situations of system (6.1). The difference is in the cases of $\delta > 0$, the limit cycle at the equator is stable while if $\delta < 0$ is unstable. This difference has a consequence of the stability type of the two equilibria at the equator after the Saddle-Node bifurcation.

6.3. **A Pitchfork bifurcation.** The second bifurcation which occurs also in all three situation of system (6.1), is a Pitchfork bifurcation. However, there is a difference between the cases of $\delta > -\beta/\omega$, $0 < \delta, -\beta/\omega$ and the cases of $\delta < 0$. In the first cases, the equilibrium which is inside the domain, collapses into the saddle-type equilibrium at the equator when $R = R_p$. After the bifurcation ($R > R_p$) a stable (with two negative eigenvalues) equilibrium is created at the equator. The flow of system (6.1) after this bifurcation is then simple. We have two equilibria at the equator, one is stable with two dimensional stable manifold and one is unstable with two dimensional unstable manifold. The flow simply moves from one equilibrium to the other. This is the end of the story for the case $\delta > -\beta/\omega$.

In the second cases ($0 < \delta < -\beta/\omega$), a saddle-type equilibrium branches out of the saddle-type equilibrium at the equator, at $R = R_p$. The equilibrium at the equator then becomes a stable equilibrium with two dimensional stable manifold.

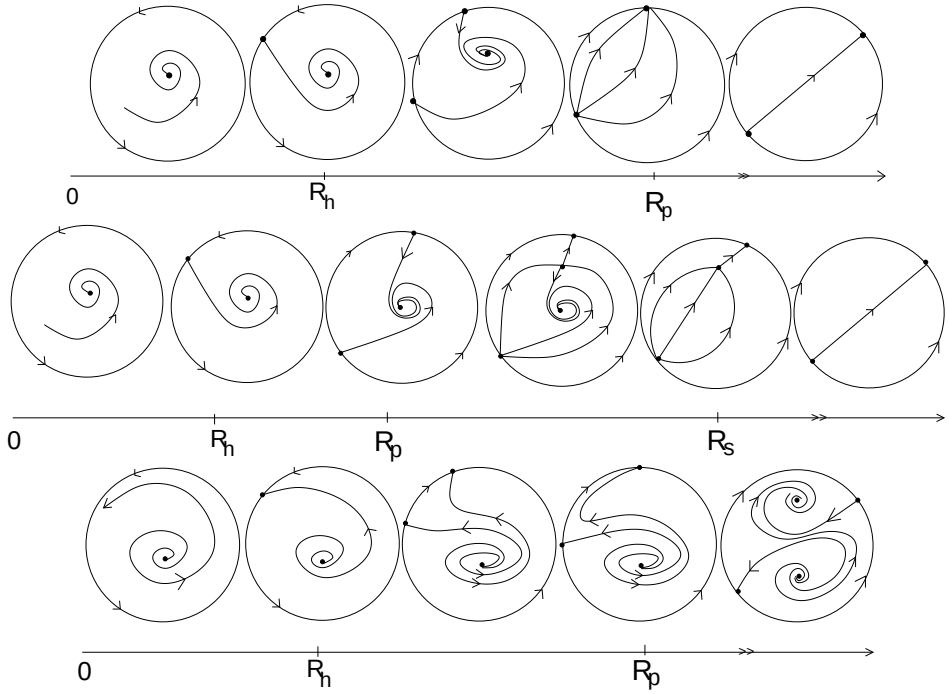

FIGURE 3. In the upper part of this figure, we present the phase portraits of system (6.1) as $R_\circ \to \infty$ for the case where $\delta > -\beta/2$. Passing through R_p, one of the equilibria of system (6.1) undergoes a Pitchfork bifurcation. As R passes through R_h we have a Saddle-Node bifurcation which happens simultaneously with a Homoclinic bifurcation. In the middle part of this figure, we draw the phase portraits of system (6.1) as $R \to \infty$ for the case where $\delta < -\beta/2$. In this case, before Pitchfork bifurcation, there is a Saddle-Node bifurcation at $R = R_s$. In the lower part of the figure, there are the phase portraits of system (6.1) in the case $\delta < 0$.

In the third cases ($\delta < 0$), a stable focus branches out of the saddle-type equilibrium at the equator. After the bifurcation, we have four equilibria, two at the equator and two inside the domain. Both of the equilibria at the equator are of the saddle type. One of the equilibria inside the domain is a stable focus while the other is unstable focus. There is no other bifurcation in the cases where $\delta < 0$.

6.4. **A Saddle-Node bifurcation.** In the cases where $0 < \delta < -\beta/\omega$ we have an extra bifurcation, i.e. a Saddle-Node bifurcation. Recall after Pitchfork bifurcation, inside the domain there is a saddle-type equilibrium. There is also a stable focus which is always there from the beginning. These two equilibria, collapses to each other in a degenerate equilibrium, if $R = R_s$. When $R > R_s$, the degenerate equilibrium vanishes. Therefore, we have a Saddle-Node bifurcation. We note that the location of the degenerate equilibrium plays an important role in the analysis of the normalized system (i.e. for $0 < \varepsilon \ll 1$). In the neighborhood of that point we find a Hopf bifurcation. See section 8.

After the bifurcation, the phase portrait of system (6.1) is again similar with the cases where $\delta > -\beta/\omega$. We are left with two equilibria at the equators, one is stable, with two dimensional stable manifold, and the other is unstable, with two dimensional unstable manifold.

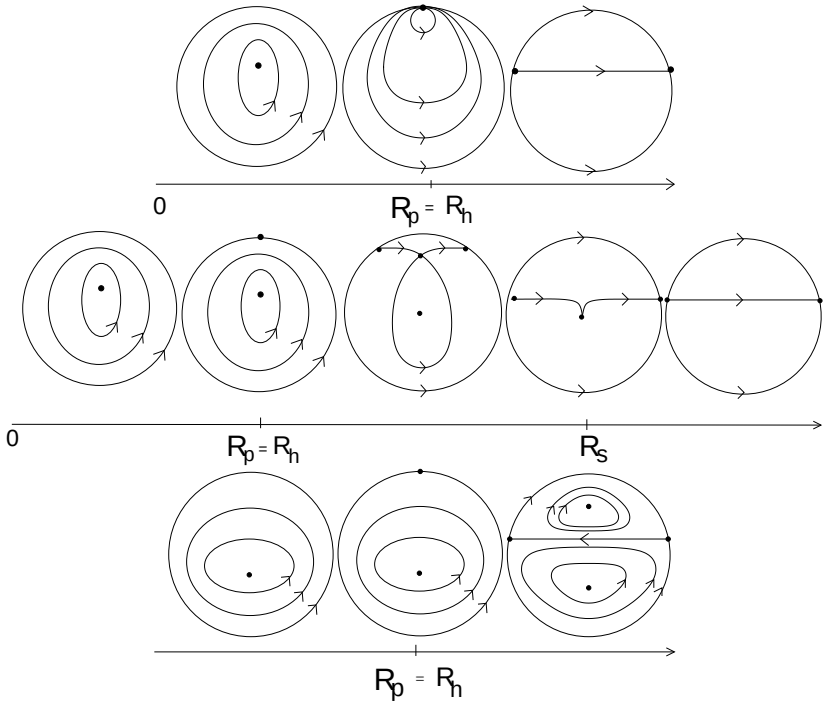

FIGURE 4. The phase portraits of system (6.1) as $R \to \infty$ for $\alpha = 0$. The upper figure is for the case where $\delta \geq -\beta/2$, the middle figure is for $0 < \delta < -\beta/2$, while the lower figure is for $\delta < 0$.

The phase portraits of system (6.1) are plotted in Figure 3.

6.5. **Some degenerate cases.** To complete the bifurcation analysis of system (6.1), let us turn our attention to the degenerate cases. We have three cases, i.e. $\alpha = 0$, $\beta = 0$, and $\delta = 0$. We only present the analysis for $\alpha = 0$. Note that if $\alpha = 0$, the vector field corresponding to system (5.1) is symmetric with respect to the y-axis. Instead of re-doing the whole calculation again, we can also draw the conclusion by looking at figure 3 and make an x-symmetric pictures out ot them. If $\alpha = 0$, we have $R_h = R_p$ which means that the linearized system of system (5.1) around the equilibrium in the equator is zero when $R = R_p$. See figure (4) for the phase-portraits of the system (6.1).

Our next goal is to turn on the perturbation ε to be non zero. Immediate consequence of this is $S(r, x, y) = {R_\circ}^2$ is no longer invariant under the flow of system (4.1).

7. The isolated nontrivial equilibrium

Let us now consider system (4.1) for $\varepsilon \neq 0$, with $\kappa_1 > 0$ and $\kappa_2 > 0$. Recall that $\dot{\mathcal{S}} = 2\varepsilon(\kappa_1 r^2 - \kappa_2(x^2 + y^2))$. Putting $\dot{\mathcal{S}} = 0$ gives us an equation which defines a cone in $\mathcal{D}$. This cone separates the phase space $\mathcal{D}$ into two parts: the *inner part* where $\dot{\mathcal{S}} < 0$ and the *outer part* where $\dot{\mathcal{S}} < 0$. If an equilibrium of system (4.1) exists, then it must lie on the cone.

The location of the nontrivial equilibrium of system (4.1) is

$$r_\circ(\varepsilon)=\sqrt{\frac{(\varepsilon^2(\beta\kappa_1-\delta\kappa_2)^2+(\varepsilon\alpha\kappa_1-\delta\omega)^2)\kappa_1\kappa_2}{((\beta\kappa_1-\delta\kappa_2)\delta)^2}}, x_\circ(\varepsilon)=-\varepsilon\tfrac{\kappa_1}{\delta}, \text{ and } y_\circ(\varepsilon)=\tfrac{(\varepsilon\alpha\kappa_1-\delta\omega)\kappa_1}{(\beta\kappa_1-\delta\kappa_2)\delta}. \tag{7.1}$$

One can immediately see that (7.1) exists if and only if $(\beta\kappa_1-\delta\kappa_2)\delta\neq 0$.

To facilitate the analysis, let us write the equilibrium (7.1) as $\boldsymbol{\xi}_\circ(\varepsilon)=(r_\circ(\varepsilon),x_\circ(\varepsilon),y_\circ(\varepsilon))$ and correspondingly, the variables $\boldsymbol{\xi}=(r,x,y)$. The variable $\boldsymbol{\xi}$, system (4.1) is written as $\dot{\boldsymbol{\xi}}=\boldsymbol{H}(\boldsymbol{\xi};\varepsilon)$. Let us also name the cone $\dot{\mathcal{S}}=\kappa_1 r^2-\kappa_2(x^2+y^2)=0$ as $\mathcal{C}$ and the set of critical points (5.4) as $\mathcal{E}$.

Assuming that $D_{\boldsymbol{\xi}}\boldsymbol{H}\left(\boldsymbol{\xi}_\circ(0)\right)$ has only one zero eigenvalue, by the Center Manifold Theorem, there exists a coordinate system such that around $\boldsymbol{\xi}_\circ(0)$, system (4.1) can be written as

$$\begin{pmatrix}\dot{\xi}_h\\ \dot{\xi}_c\end{pmatrix}=\begin{pmatrix}A(\varepsilon)\xi_h\\ \lambda(\varepsilon)\xi_c\end{pmatrix}+\text{higher-order term}, \tag{7.2}$$

where $A(0)$ has no zero eigenvalue and $\lambda(0)=0$. Let us choose ε_1 small enough such that the eigenvalues of $A(\varepsilon)$ remain non zero for $0<\varepsilon\leq\varepsilon_1$.

Let W_ε be the invariant manifold of system (7.2) which is tangent to $E_{\lambda(\varepsilon)}$ at $\boldsymbol{\xi}_\circ(\varepsilon)$, where $E_{\lambda(\varepsilon)}$ is the linear eigenspace corresponding to $\lambda(\varepsilon)$. We note that the Center Manifold Theorem gives the existence of W_ε. Also, W_0 is the center manifold of $\boldsymbol{\xi}_\circ(0)$, which is, in our case, uniquely defined and tangent to $\mathcal{E}$ at $\boldsymbol{\xi}_\circ(0)$. Since $\mathcal{E}$ intersects $\mathcal{C}$ at $\boldsymbol{\xi}_\circ(0)$ transversally, for small enough ε_2 we have $W_c(\varepsilon)$ intersect $\mathcal{C}$ at $\boldsymbol{\xi}_\circ(\varepsilon)$ transversally for $0<\varepsilon\leq\varepsilon_2$.

Lastly, $\mathcal{E}$ also intersects $S(R)$ transversally, for $|R-\parallel\boldsymbol{\xi}_\circ(0)\parallel|<c$ for some positive number c. This follows from the assumption that $D_{\boldsymbol{\xi}}\boldsymbol{H}\left(\boldsymbol{\xi}_\circ(0)\right)$ has only one zero eigenvalue. Thus, there exists ϵ_3, small enough, such that $W_c(\varepsilon)$ intersects $S(R)$ transversally for $|R-\parallel\boldsymbol{\xi}_\circ(\varepsilon)\parallel|<c$ and $0<\varepsilon\leq\varepsilon_3$. Choosing $\varepsilon^*=\min\{\varepsilon_1,\varepsilon_2,\varepsilon_3\}$, we have proven the following lemma.

Lemma 7.1. *Let us assume that $D_{\boldsymbol{\xi}}\boldsymbol{H}\left(\boldsymbol{\xi}_\circ(0)\right)$ has only one zero eigenvalue. There exists $0<\varepsilon^*\ll 1$ such that, for $\varepsilon\in(0,\varepsilon^*)$, the system (7.2) has an invariant manifold W_ε which is tangent to $E_{\lambda(\varepsilon)}$ at $\boldsymbol{\xi}_\circ(\varepsilon)$. This invariant manifold intersects the cone $\dot{\mathcal{S}}=0$ transversally at $\boldsymbol{\xi}_\circ(\varepsilon)$. It also intersects the sphere $S(R)$ transversally, for all R, $|R-\parallel\boldsymbol{\xi}_\circ(0)\parallel|<\varepsilon$.*

From system (7.2), we conclude that the dynamics in the manifold W_ε is slow since $\lambda(\varepsilon)=O(\varepsilon)$ if $\varepsilon\in(0,\varepsilon^*)$. The Lemma 7.1 also gives us the stability result for the equilibrium (7.1). If $\varepsilon\in[0,\varepsilon^*)$, then the eigenvalues of $A(\varepsilon)$ remain hyperbolic. Thus, we can use the analysis in section 4. For the sign of $\lambda(\varepsilon)$ we have the following lemma.

Lemma 7.2. *Consider the system (7.2). For $\varepsilon\in(0,\varepsilon^*)$, we have $\lambda(\varepsilon)>0$ if*

(1) *$\delta<0$ and $\kappa_2\delta>\kappa_1\beta$, or*
(2) *$-\beta\kappa_1/(2\kappa_1+\kappa_2)<\delta<-\beta/2$.*

Also for $\varepsilon\in(0,\varepsilon^*)$, $\lambda(\varepsilon)<0$ if

(1) *$\delta<0$ and $\kappa_2\delta<\kappa_1\beta$, or*
(2) *$\delta\geq-\beta/2$, or $0<\delta<-\beta\kappa_1/(2\kappa_1+\kappa_2)$.*

Proof. We only prove the first case of the first part of the lemma. The other cases can be proven in the same way. From Lemma 7.1, we conclude that W_ε intersects the cone $\mathcal{C}$ transversally. The situation for $\delta<0$, $\beta<0$, and $\kappa_2\delta>\kappa_1\beta$, is drawn in figure 5. The three

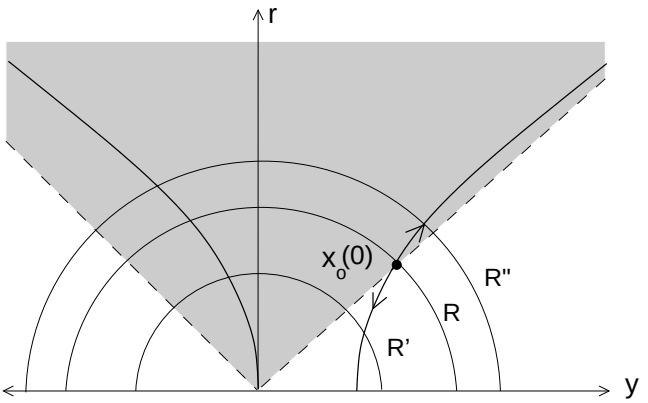

FIGURE 5. The continuous set of critical points $\mathcal{E}$ for $\delta < 0$ and $\beta < 0$ is plotted on the figure above. The dashed lines represent the cone $\mathcal{C}$. It separates the phase-space into two parts, the expanding part (the shadowed area) and the contracting part. There are also three concentric circles drawn in this figure. The radius of these circles satisfies: $R' < R < R''$.

concentric circles, marked by R', R and R'', are the intersection between the sphere $S(R')$, $S(R)$, and $S(R'')$ with the plane $x = 0$ (respectively). Note that $\max\{|R'-R|, |R''-R'|, |R''-R|\} < \varepsilon$. As ε becomes positive, an open subset of $\mathcal{E}$ which contains $\boldsymbol{\xi}_\circ$ can be continued with ε and form the invariant slow manifold W_ε with properties described in Lemma 7.1. Thus, we conclude that inside the shadowed area, the dynamics is moving from $S(R)$ to $S(R'')$. On the other side, the dynamics is moving from $S(R)$ to $S(R')$, i.e. $\lambda(\varepsilon) > 0$. □

In section 4 we left out a question: whether the solutions of system (4.1) are bounded in the case $\delta < 0$. Using the same arguments as in Lemma 7.1 and the proof of lemma 7.2, for ε small enough we have the following result.

Corollary 7.3. *If $\delta < 0$, $\alpha < 0$ and $\kappa_2\delta < \kappa_1\beta$ then the solution of (4.1) is bounded.*

Proof. If $\delta < 0$, $\mathcal{E}$ is a hyperbola with two branches: the negative and positive branches. The negative branch is the one that passes through the origin. For $\alpha < 0$, the positive branch is attracting. Moreover, the positive branch is in the interior of $\dot{\mathcal{S}} < 0$. This ends the proof. □

In the next section we are going to study the behavior near the boundary $\kappa_2/\kappa_1 = (\beta\delta - 2(\delta+\beta))/\delta$.

8. Hopf bifurcations of the nontrivial equilibrium

The most natural thing to start with in doing the bifurcation analysis is to follow an equilibrium while varying one of the parameters in system (4.1). However, the analysis in the previous sections shows that we have no possibility of having more than one nontrivial critical point. Thus, we have excluded the Saddle-Node bifurcation of the nontrivial equilibrium of our system. Let us fix all parameters but δ. We will use this parameter as our continuation parameter. Recall that we have fixed $\beta < 0$, $\alpha < 0$, $\omega > 0$ and $\kappa_j > 0, j = 1, 2$.

Let $\delta > -\beta\kappa_1/(2\kappa_1 + \kappa_2)$ and consider the system (7.2). By Lemma 5.2, considering the chosen value of parameters: $\beta < 0$, $\alpha < 0$, $\omega > 0$ and $\kappa_j > 0, j = 1, 2$, we conclude that

$\Re(\lambda_{1,2}) < 0$, where $\lambda_{1,2}$ are the eigenvalues of $A(0)$. Using Lemma 7.1, for small enough ε, $\Re(\lambda_{1,2}(\varepsilon)) < 0$ where $\lambda_{1,2}(\varepsilon)$ are the eigenvalues of $A(\varepsilon)$. If $\delta < -\beta\kappa_1/(2\kappa_1 + \kappa_2)$, by Lemma 7.1 we have $\lambda(\varepsilon) > 0$ and by Lemma 5.2, we have $\lambda_3 > 0$.

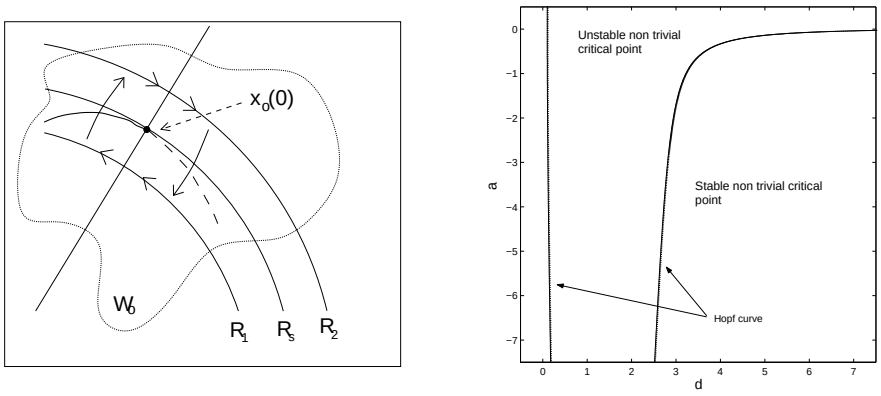

FIGURE 6. In the left figure we draw the illustration for the situation in Theorem 8.1. $W_\circ$ is the center manifold of $\boldsymbol{\xi}_\circ(0)$. The three curves labelled by R_1, R_2 and R_s are the intersection between the center manifold W_ε with $S(R)$, where the label is the value of R. In the right figure, we plot the two parameters numerical continuation of the Hopf point that we found if $\delta > 0$. The numerical data for this continuation are: $\beta = -6$, $\omega = 3$, $\kappa_1 = 5$, $\kappa_2 = 1$ and $\varepsilon = 0.01$.

See the left figure of figure 6 where we have drawn an illustration for this situation. At $\delta = -\beta\kappa_1/(2\kappa_1 + \kappa_2)$ we have the situation where system (4.1) near $\boldsymbol{\xi}_\circ(0)$ has a two-dimensional center manifold W_ε. Locally, $W_\circ$ intersect $S(R_s)$ transversally (thus, so does W_ε for small enough ε). At $S(R_2)$, the analysis in the section 6 shows that there are only two equilibria which are at the equator. It is easy to check that the dynamics is as depicted in Figure 6. At $S(R_1)$, as a equilibrium of system (6.1), $\boldsymbol{\xi}_\circ(0)$ has undergone a Saddle-Node bifurcation. Thus, it splits up into one stable equilibrium and one saddle type equilibrium, which are drawn using a solid line and a dashed line respectively. Again, the dynamics at $S(R_1)$ is then verified. For $\varepsilon \neq 0$ but small, all of the dynamics is preserved. As an addition, we pick up a slow dynamics moving from one sphere to the other which is separated by the cone $\mathcal{C}$ which is the straight line in Figure 6. This geometric arguments show that in the center manifold W_ε, around $\boldsymbol{\xi}_\circ(\varepsilon)$, we have rotations. Thus, as δ passes $-\beta\kappa_1/(2\kappa_1 + \kappa_2)$, generically the nontrivial equilibrium undergoes a Hopf bifurcation.

Theorem 8.1 (Hopf bifurcation I)**.** *Keeping $\beta < 0$, $\alpha < 0$, $\omega > 0$ and $\kappa_j > 0, j = 1, 2$ fixed, the nontrivial equilibrium (7.1) undergoes a Hopf Bifurcation in the neighborhood of $\delta = -\beta\kappa_1/(2\kappa_1 + \kappa_2)$.*

Remark 8.2. *It is suggested by this study that if we singularly perturbed a Saddle-Node bifurcation we get a Hopf bifurcation. One could ask a question how generic is this phenomena. The answer to this question can be found in the seminal paper of M. Stiefenhofer* [19]*. Using blown-up transformations with different scaling (this is typical in singular perturbation problems), it is proved that this phenomenon is generic.*

We check this with numerical computation for the parameter values: $\alpha = -2$, $\beta = -6$, $\omega = 3$, $\kappa_1 = 5$, $\kappa_2 = 1$ and $\epsilon = 0.01$. We found Hopf bifurcation in the neighborhood of $\delta = 2.81$ while our analytical prediction is 2.73. We have to note that from our analysis it seems that the parameter α does not play any role. However, the location of the nontrivial equilibrium depends on α. This might be the explanation for the rather large deviation of our analytical prediction of the bifurcation value δ, compare to the numerical result.

We can also vary κ_1 while keeping δ fixed. Again, we find an agreement with our analytical prediction. In this experiment, we kept $\alpha = -2$, $\beta = -6$, $\omega = 3$, $\kappa_2 = 1$ and $\epsilon = 0.01$. For $\delta = 2$ we found Hopf bifurcation if $\kappa_1 \approx 0.9342573$ (predicted by Theorem 8.1 at $\kappa_1 = 1$). If $\delta = 1.5$, we found $\kappa_1 \approx 0.4861231$ (predicted at $\kappa_1 = 0.5$) and if $\delta = 1$ at $\kappa_1 \approx 0.2472450$ (predicted at $\kappa_1 = 0.25$).

Another Hopf bifurcation happens in the neighborhood of $\alpha = 0$. This is obvious from the bifurcation analysis of the system (6.1). We have the following result.

Theorem 8.3 (Hopf bifurcation II)**.** *If $\delta < 0$ or if $\delta > -\beta/2$, keeping all other parameter fixed but α, the nontrivial equilibrium (7.1) undergoes a Hopf Bifurcation in the neighborhood of $\alpha = 0$.*

On the left figure of Figure 6, we have plotted a two parameters continuation of the Hopf point in (α, δ)-plane. One can see that for a large value of δ, Hopf bifurcation occurs in the neighborhood of $\alpha = 0$. This is in agreement with Theorem 8.3. For $\delta < \beta/2 \approx 3$ in our experiment, the Hopf curve is almost independent of α just as it is predicted by Theorem 8.1. We find also another Hopf bifurcation close to $\delta = 0$. This branch is actually belong to the same curve. However, to see this bifurcation we need to re-scale the parameter which results in a different asymptotic ordering. We are not going into the details of this.

9. Numerical continuations of the periodic solution

In this section we present a one parameter continuation of the periodic solution created via Hopf bifurcation of the nontrivial critical point. This is in general a difficult task to do analytically. Using the numerical continuation software AUTO [5], we compute the one parameter continuations of the periodic solution.

9.1. **A sequence of Period-Doubling and Fold bifurcations.**

The numerical data that we use are the same as in the previous section: $\alpha = -2$, $\beta = -6$, $\omega = 3$, $\kappa_1 = 5$, $\kappa_2 = 1$ and $\epsilon = 0.01$. We start with a stable equilibrium found for $\delta = 4$ and follow it with decreasing δ. Recall that in the neighborhood of $\delta = 2.81$ we find a Hopf bifurcation where a periodic solution is created.

We follow this periodic solution with the parameter δ. The periodic solution undergoes a sequence of Period-Doubling and Fold bifurcations. In figure 7 we plot δ against the period of the periodic solution. Also we attached the graph of the periodic solutions. For δ in the neighborhood of 1.15, the periodic solution is unstable (except probably in some very small intervals of δ). Moreover, the trivial and the nontrivial equilibria are also unstable. Since the solution is bounded, by forward integration we will find an attractor. We plotted the attractor and the Poincaré section of the attractor in the same figure.

The attractor that we found by forward integrating is non-chaotic. All of its Lyapunov multipliers are negative. It is not clear at the moment whether the attractor is periodic or not. The Poincaré section that we draw suggests that this is not a periodic solution.

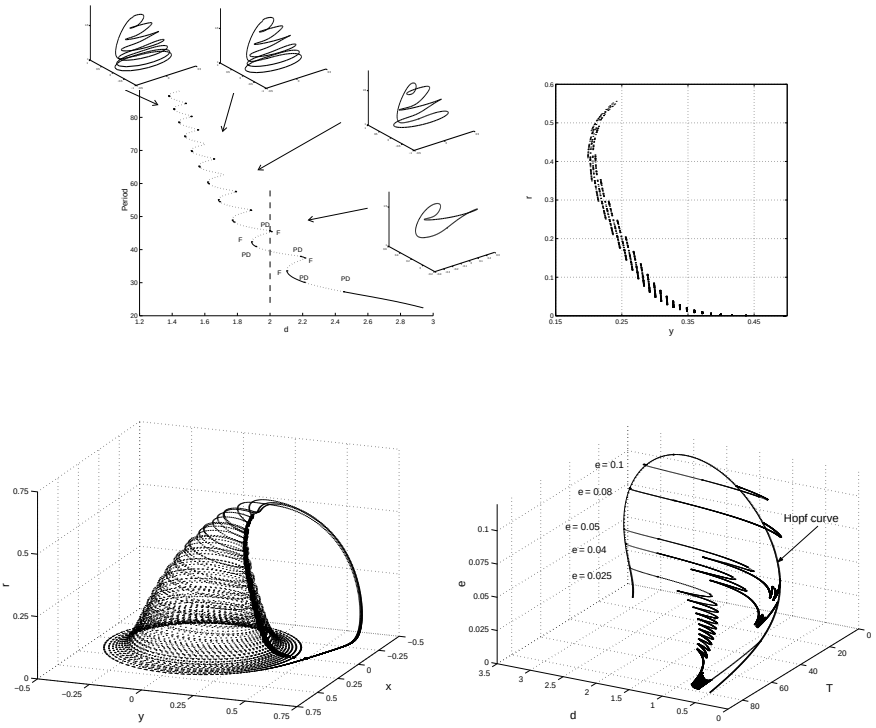

FIGURE 7. On the upper-left part of this figure we plot the sequence of Period-Doubling and Hopf bifurcations of the periodic solution. There also we have attached the periodic solution for four decreasing values of δ. The attractor for $\delta = 1.1$ is drawn in the lower-left part of of this figure while in the upper-right part is the the Poincaré section of the attractor. The numerical data that we use are $\alpha = -2$, $\beta = -6$, $\omega = 3$, $\kappa_1 = 5$, $\kappa_2 = 1$ and $\epsilon = 0.01$. On the lower-right part of the figure, we plot the two parameters continuation of the Hopf point using ϵ and δ. For several values of ε, we do one parameter continuation of the resulting periodic solution.

Although a sequence of Period-Doubling and Fold bifurcations usually leads to chaos, it seems that in our system it is not the case. In order to understand this, we do two parameters continuation of the Hopf point. The parameters that we use are δ and ε. Recall that we have fixed $\alpha = -2$, $\beta = -6$, $\kappa_1 = 5$, and $\kappa_2 = 1$.

In figure 7, we also plotted the result of two parameters continuation of the Hopf point using δ and ε. One can see that as the value of ε increases, the distance between two Hopf bifurcations in parameter space becomes smaller. The periodic solution that comes out of the nontrivial equilibrium via the first Hopf bifurcation, collapses back into the nontrivial equilibrium via another Hopf bifurcation. For several values of ε we plot the one parameter continuation of the periodic solution. This result gives us an indication that the sequence of Period-Doubling and Fold bifurcations in our case is not an infinite sequence. We remark though that it is still possible that for ε small enough, we might still find an infinite sequence of these bifurcations. We do not have that for $\varepsilon \geq 0.025$.

Remark 9.1. *It is also interesting to note that, based on these numerical studies, there is an indication that the behavior of the system (4.1) is actually much simpler if μ_1 and μ_2 are*

large. This observation is based on the fact that for $\varepsilon > 0.114$, the nontrivial equilibrium is stable. The flow then collapses into this critical point, except inside the invariant manifold $r = 0$.

9.2. **The slow-fast structure of the periodic solution.** Let us now try to understand

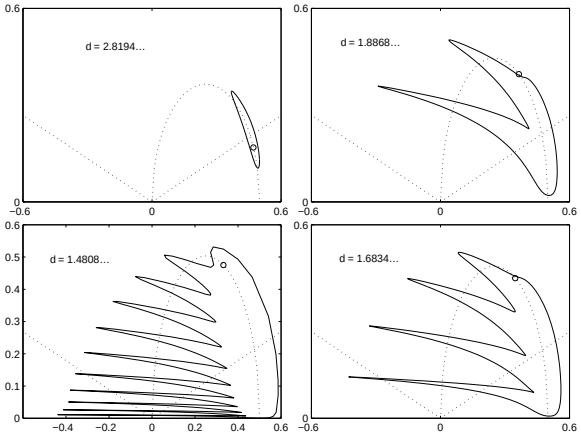

FIGURE 8. In this figure we plot the projections to the (y, r)-plane of the periodic solution for four different values of δ.

the construction of this periodic solution. From the previous discussion, one can see that exactly at the Hopf bifurcation point, the center manifold of the corresponding equilibrium is not tangent to the sphere $S(R)$. This means that the periodic solution that is created after the bifurcation is a combination of slow and fast dynamics.

In figure 8 we have plotted the projections to the (r, y)-plane of the periodic solution for four values of δ. On each plot, there are two dotted lines through the origin. These lines represent the cone $\mathcal{C}$. Thus, the location of the nontrivial equilibrium is in $O(\varepsilon)$-neighborhood of the intersection point between one of the lines with the ellipse $\mathcal{E}$.

This periodic solution is created via Hopf bifurcation at $\delta \approx 2.81$. We draw the projection of the periodic solution at four values of δ, i.e. $2.8194\ldots$, $1.8868\ldots$, $1.6834\ldots$ and $1.4808\ldots$. We also plotted the ellipse of equilibria and the cone $\dot{\mathcal{S}} = 0$ using dotted lines. As δ decreases, the periodic solution gets more loops which is represented by the spikes in figure 8. This fits our analysis in section 6 (see also figure 3). For $\varepsilon = 0$ and $R > 0$ small enough, the equator of the sphere $r^2 + x^2 + y^2 = R^2$ is an unstable periodic solution of system (5.1), since $\alpha < 0$. However, the equator become less unstable when δ decreases (recall that the stability of the equator is determined by $\alpha\delta$, see (6.3)). Thus, the smaller δ is, the longer the periodic solution stays near the invariant manifold $r = 0$.

Recall that as δ decreases, the periodic solution described above also undergoes a sequence of Period-Doubling and Fold bifurcations. Thus, apart from the periodic solution above, there is also some unstable periodic solutions with much higher period. Moreover, the periodic solution that we plotted in figure (8) is not necessarily stable.

9.3. **Non-existence of orbits homoclinic to the origin.** In the system (4.1), the condition on the saddle value to have Shilnikov bifurcation can be easily satisfied (see [9] for the

condition). However, we cannot have a homoclinic orbit in the normal form. The reason is quite straightforward. In Theorem 3.1 we prove that the plane $r = 0$ is invariant under the flow of the normal form. It implies that the two-dimensional stable manifold of the equilibrium at the origin is $r = 0$. Thus, there is no possibility of having an orbit homoclinic to this critical point.

Moreover, we can not perturb the manifold away by including the higher order terms in the normal form. The existence of an orbit homoclinic to the origin in the full system is still an open question, which is not treated in this paper. Another possibility is to add some term that perturbed the invariant manifold $r = 0$ away. This can be done by introducing time dependent perturbation, for instance: periodic forcing term or parametrically excited term. These are subjects of our further research.

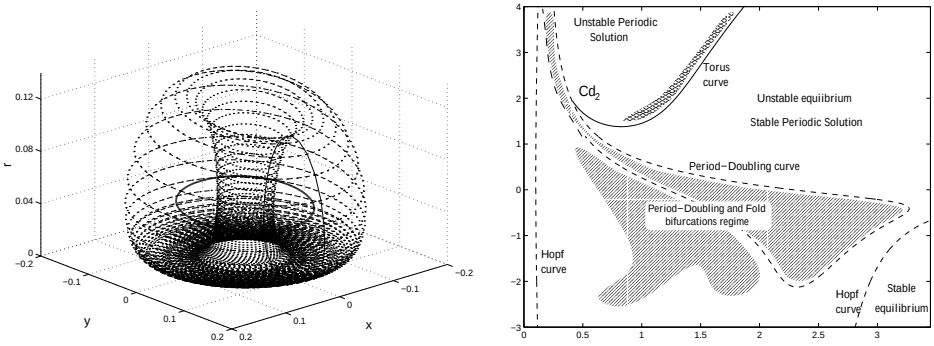

FIGURE 9. In this figure, on the left part we plot the Torus that we find by continuing a periodic solution. This periodic solution is created via Hopf bifurcation at $\delta = 2.81$ and $\alpha = -2$. The torus is computed for the value of $\alpha = 6.8$. On the rigth-hand side, we plot the two parameters continuation of the Torus bifurcation point, Hopf point and one branch of the Period-Doubling point. The vertical axis is α while the horizontal is δ.

9.4. **Torus bifurcation.** Another interesting bifurcation that happens in system (2.3) is a Torus bifurcation. This bifurcation is found by following the periodic solution which is created after Hopf bifurcation. Recall that the numerical data that we use are $\alpha = -2$, $\beta = -6$, $\omega = 3$, $\kappa_1 = 5$, $\kappa_2 = 1$ and $\epsilon = 0.01$. At $\delta = 2.81$ we find a Hopf bifurcation, and if we continue the periodic solution by varying δ, we get a sequence of Fold and Period-Doubling bifurcations as drawn in figure 7.

Instead of following the stable periodic solution with δ, we now follow it using α. Around $\alpha = -0.9$, the periodic solution becomes unstable via Period-Doubling bifurcation. Around $\alpha = -0.2$, the periodic re-gain its stability by the same bifurcation. Around $\alpha = 6.7$, the periodic solution becomes neutrally stable. After this bifurcation, an attracting torus is created and it is drawn in figure 9 on the left. This is also known as *Secondary Hopf* or Neimark-Sacker bifurcation. See [13].

To complete the bifurcation analysis, in the same figure but on the right, we plot the two parameter continuation of the Torus bifurcation, the Hopf bifurcation and the two Period Doubling bifurcations mentioned above. Note that the two Period-Doubling bifurcations are actually connected. On that diagram we have indicated the region where we have a stable nontrivial critical point. Above the Torus curve (the curve where the periodic solution

becomes neutrally stable), we shaded a small domain. In that domain, we can expect to compute the torus numerically.

Further away from the curve, the torus get destroyed and a new attractor is formed. The reason for this destruction is since the location of the torus is quite close to the invariant manifold $r = 0$. Recall that the closer we are to the invariant manifold, the more we get attracted to the origin. This is why the torus is destroyed.

The torus curve ends in co-dimension two point Cd_2. There is still a lot of work that have to be done to be able to say something more about the the behaviour near this point. We are not going to do that in this paper. Also, near this point there is a lot of Period-Doubling and Fold curves which are close to each other in the (δ, α)-plane. It is indeed interesting to devote some studies to the neighborhood of point Cd_2.

Remark 9.2. *In doing the numerical continuation, we found that to compute the three-dimensional torus in our system is cumbersome. The computation become less cumbersome if the value of κ_1/κ_2 is not large. For instance, our computation which results are plotted in Figure (9) is for $\kappa_1/\kappa_2 = 5$. If we decrease this value, it is easier to compute the torus since it survives in a larger set of parameters.*

9.5. **A heteroclinic connection.** For $\delta < 0$, the nontrivial equilibrium undergoes a Hopf bifurcation in the neighborhood of $\alpha = 0$. Continuing this periodic solution using α as the continuation parameter, we find a Torus bifurcation. Apart from this bifurcation, we do not find another codimension one bifurcation of the periodic solution.

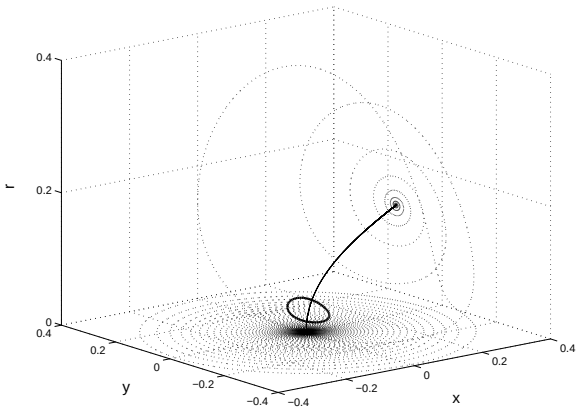

FIGURE 10. Heteroclinic connection between the nontrivial and the trivial equilibria. We plot also the attracting periodic solution by a thick line.

If $\alpha < 0$, in the previous analysis we show that negative branch of the hyperbola is repelling. If we choose, $\kappa_2\delta < \kappa_1\beta$, by Corollary 7.3 we conclude that the solutions of system (2.3) are bounded. The trivial and the nontrivial equilibria are both unstable of the saddle type. The trivial equilirbium has two-dimensional stable manifold W_s^o (which is $r = 0$) and one dimensional unstable manifold which is exponentially close to the negative branch. On the other hand, the nontrivial equilibrium has two-dimensional unstable manifold W_u^n which is locally transversal to the negative branch, and one dimensional stable manifold which is exponentially close to the negative branch.

Generically, W_s^o intersects W_u^n transversally in a one-dimensional manifold. This one-dimensional manifold lies in $r = 0$. However, in our system there is no other limit set in

$r = 0$ appart from the origin. Thus, we conclude that the two manifolds do not intersect each other. Since the solutions are bounded, we conclude that W_u^n does not span to infinity. By these arguments, we numerically find an attracting periodic solution to where the W_u^n is attracted to. Moreover, the one-dimensional unstable manifold of the origin, is connected with the one-dimensional stable manifold of the nontrivial critical point. We illustrate the situation in Figure 10.

10. Concluding remarks

We have discussed in this paper the dynamics of a four-dimensional system of coupled oscillators with widely separated frequencies. In combination with an energy-preserving nonlinearity, it creates a system with rich dynamics of the slow-fast type in three-dimensional space. We do not claim that we have completed the analysis of the dynamics of such a system. However, in this paper we have presented a large part of it. The normal form of our system can be viewed as a three-dimensional energy-preserving system which is linearly perturbed. The flow of the energy-preserving part lives in two dimensional integral manifolds. These manifold fiber the phase-space.

We have completed the analysis for the energy-preserving part of the normal form. Although in a sense it is very special, we note that the energy-preserving part can be viewed as a Bounded-Quadratic-Planar system which has been extensively studied but still contains a lot of open problems. Extending this analysis for small perturbations, we can get a lot of information of the normal form.

Although we leave out the forcing terms, there is energy exchange between the characteristic modes of our normal form. The main ingredient that we need for this energy exchange is $\mu_1\mu_2 < 0$. Physically, this means one of the modes should be damped while the other is excited. This, however, is not a restrictive condition since if both modes are damped (or excited), clearly one would need an energy source (or an absorber) to have energy exchange.

In relation with the results in [8, 23] on how to prove that a three-dimensional system of differential equations is non-chaotic, we note that our system is more complex than theirs. The studies in [8, 23] are concentrated on nonlinear three-dimensional systems having only at most 5 terms. Our normal form contains 11 terms. So far in our analysis we find no trace of chaotic behavior. It is evident in our system that we cannot have homoclinic orbits. This excludes the Shilinkov's scenario for a route to chaos. Thus, whether our system is chaotic or not is still an open question. It is also interesting to note that Torus (or Neimark-Sacker) bifurcation usually is followed by a lot of chaos in the system, in the presence of homoclinic tangencies (see for instance [3]). This may provide us with a way to find chaotic behavior in our system.

We leave out several interesting questions from our analysis. Below we have listed several open questions.

(1) The invariant manifold $r = 0$ can be perturbed away by perturbing the systems with small periodic forcing term or a parametrical excitation term. In the absence of this invariant manifold, we might find homoclinic orbit that could lead to a lot of interesting dynamics. The complication is, we have to analyze a 4-dimensional normal form.

(2) The behavior (dynamics) of the system near the co-dimension two point: Cd_2 is not analyzed in this paper. This type of co-dimension two point is treated carefully in the book by Kuznetsov [13]. One could for instance follow the periodic solution around the point Cd_2 and compare the result with those studies in [13].
(3) The global dynamics in the case of the absence of the nontrivial equilibrium is also an interesting case. This will be treated in a sequel of this paper.

Acknowledgment. J.M. Tuwankotta wishes to thank KNAW and CICAT TUDelft for financial support. He wishes to thank Hans Duistermaat, Ferdinand Verhulst (both from Universiteit Utrecht) and Daan Crommelin (Universiteit Utrecht and KNMI) from Universiteit Utrecht for many discussions during this research. Also to Yuri Kuznetsov, Bob Rink, Thijs Ruijgrok and Lennaert van Veen (all from Universiteit Utrecht) for many comments. He also thanks Santi Goenarso for her support in various ways.

References

[1] Broer, H.W., Chow, S.N., Kim, Y., Vegter, G., *A normally elliptic Hamiltonian bifurcation*, ZAMP 44, pp. 389-432, 1993.
[2] Broer, H.W., Chow, S.N., Kim, Y., Vegter, G., *The Hamiltonian Double-Zero Eigenvalue*, Fields Institute Communications, vol. 4, pp. 1-19, 1995.
[3] Broer, H.W., Simó, C., Tatjer, J. C. *Towards global models near homoclinic tangencies of dissipative diffeomorphisms.*, Nonlinearity 11, no. 3, pp. 667-770, 1998.
[4] Crommelin, D.T.*Homoclinic Dynamics: A Scenario for Atmospheric Ultralow-Frequency Variability*, Journal of the Atmospheric Sciences, Vol. 59, No. 9, pp. 1533-1549, 2002.
[5] Doedel, E., Champneys, A., Fairgrieve, T., Kuznetsov, Y., Sandstede, B., Wang, X.-J, *AUTO97: Continuation and bifurcation software for ordinary differential equations (with HomCont)*, Computer Science, Concordia University, Montreal Canada, 1986.
[6] Dumortier, F., Herssens, C., Perko, L.,*Local bifurcations and a survey of bounded quadratic systems*, J. Differential Equations 165 (2000), no. 2, 430–467.
[7] Fenichel, N., *Geometric Singular Perturbation Theory for Ordinary Differential Equations*, Journal of Differential Equations 31, pp. 53-98, 1979.
[8] Fu, Zhang, Heidel, Jack, *Non-chaotic behaviour in three-dimensional quadratic systems*, Nonlinearity 10, no. 5, pp. 1289-1303, 1997.
[9] Guckenheimer, J., Holmes, P.H., *Nonlinear Oscillations, Dynamical Systems, and Bifurcations of Vector Fields*, Applied Math. Sciences 42, Springer-Verlag, 1997.
[10] Haller, G., *Chaos Near Resonance*, Applied Math. Sciences 138, Springer-Verlag, New York etc., 1999.
[11] Hirsch, M. W., Pugh, C. C., Shub, M., *Invariant manifolds.*, Lecture Notes in Mathematics, Vol. 583, Springer-Verlag, Berlin-New York, 1977.
[12] Jones, C.K.R.T., *Geometric singular perturbation theory*, in Dynamical Systems, Montecatibi Terme, Lecture Notes in Math. 1609, ed. R. Johnson, Springer-Verlag, Berlin, pp. 44-118, 1994.
[13] Kuznetsov, Yuri A., *Elements of applied bifurcation theory*, second edition, Applied Mathematical Sciences, 112. Springer-Verlag, New York, 1998.
[14] Langford, W.F., Zhan, K.,*Interactions of Andonov-Hopf and Bogdanov-Takens Bifurcations*, Fields Institute Communications, vol. 24,pp. 365-383, 1999.
[15] Langford, W.F., Zhan, K.,*Hopf Bifurcations Near* 0 : 1 *Resonance*, BTNA'98 Proceedings, eds. Chen, Chow and Li, pp. 1-18, Springer-Verlag, New York etc., 1999.
[16] Nayfeh, S.A., Nayfeh, A.H., *Nonlinear interactions between two widely spaced modes-external excitation*, Int. J. Bif. Chaos 3, pp. 417-427, 1993.

[17] Nayfeh, A.H., Chin, C.-M., *Nonlinear interactions in a parametrically excited system with widely spaced frequencies*, Nonlin. Dyn. 7, pp. 195-216, 1995.
[18] Sanders, J.A., Verhulst, F., *Averaging Method on Nonlinear Dynamical System*, Applied Math. Sciences 59, Springer-Verlag, New York etc., 1985.
[19] Stiefenhofer, Matthias, *Singular perturbation with limit points in the fast dynamics*, Z. Angew. Math. Phys. 49 (1998), no. 5, 730-758.
[20] Tuwankotta, J.M., Verhulst, F., *Hamiltonian Systems with Widely Separated Frequencies*, Preprint Universiteit Utrecht no. 1211, 2001.
[Online] `http://www.math.uu.nl/publications/preprints/1211.ps.gz`.
[21] Verhulst, F., A Workbook on Singular Perturbations, Universiteit Utrecht.
[22] Wiggins, Stephen, *Normally hyperbolic invariant manifolds in dynamical systems*, with the assistance of György Haller and Igor Mezić. Applied Mathematical Sciences, 105. Springer-Verlag, New York, 1994.
[23] Yang, Xiao-Song, *A technique for determining autonomous 3-ODEs being non-chaotic*, Chaos Solitons Fractals 11, no. 14, pp. 2313–2318, 2000.

E-MAIL: TUWANKOTTA@MATH.UU.NL, MATHEMATISCH INSTITUUT, UTRECHT UNIVERSITY, PO BOX 80.010, 3508 TA UTRECHT, THE NETHERLANDS; ON LEAVE FROM JURUSAN MATEMATIKA, FMIPA, INSTITUT TEKNOLOGI BANDUNG, GANESHA NO. 10, BANDUNG, INDONESIA